An empirical probabilistic study of wind direction over complex terrain

Sharples, J.J. [1], R.H.D. McRae [2, 3] and R.O. Weber [1, 3]

[1] *School of Physical Environmental and Mathematical Sciences University of New South Wales at the
Australian Defence Force Academy, Australian Capital Territory*
[2] *Emergency Services Agency, Curtin, Australian Capital Territory*
[3] *Bushfire Cooperative Research Centre, Melbourne, Victoria*
Email: *j.sharples@adfa.edu.au*

Abstract: Understanding spatially distributed wind fields over complex terrain is important for a variety of applications including pollutant dispersion modelling and light and recreational aviation as well as the interdependent problems of fire spread modelling and bushfire risk management. Directional changes in surface winds are particularly important in this latter context. To accurately predict the spread of a fire, models often incorporate methods to account for modifications in the surface wind field driven by interactions with the terrain. The simplest of these methods assume a single wind speed and direction over the whole region of interest. While such an assumption may be valid over flat or slightly undulating terrain and may even be able to account for large-scale fire spread patterns in more mountainous terrain, finer-scale processes that can have a significant role on fire severity and in the risk of fire escalation will not be properly represented. These include finer-scale processes such as the interaction of bushfire with channelled flows and lee-slope eddies, which can have a significant effect of the ecological and hydrological aspects of bushfire risk, for example, as well as the risk a bushfire poses to life and property.

More sophisticated methods include deriving a terrain-modified wind field using computational fluid dynamics (CFD), mass consistency or empirically derived look-up tables. These methods are inherently deterministic in nature, producing a unique terrain-modified wind field for a given ambient wind vector. While these methods can offer significant improvements in predicting the evolution of fire perimeters, they are typically more computationally intensive and can fail to recognise the nonlinear and thermal effects that the terrain can have on local winds. Moreover, such methods can be difficult to validate over large tracts of land.

In this paper we discuss an alternative method for understanding the directional aspect of wind-terrain systems. Terrain-modified winds are analysed using joint probability distributions derived from wind speed and direction data collected in the Tidbinbilla Nature Reserve in the southwest of the Australian Capital Territory. Empirical distributions of wind direction are used to identify and characterise the dominant states of the particular wind-terrain system, in this case a steep east-facing slope. By considering the modal structure of joint distributions relating the conditional probability of different terrain-modified wind responses over the spectrum of ambient (input) wind vectors, several important wind-terrain interactions are identified and discussed. By analysing the temporal characteristics of data comprising particular modes a number of particular processes including thermally forced winds, lee-slope eddies and dynamic channelling are identified. The method discussed offers a way of characterising terrain-modified winds in terms of likelihood, which may be better suited to risk-based approaches to bushfire management in high-country or mountainous landscapes. The analyses also reveal the inherently stochastic nature of the wind-terrain system, and thus raise some doubts about the suitability of deterministic approaches to modelling terrain-modified surface winds in rugged terrain.

Keywords: *Wind direction, complex terrain, channelling, thermal winds, lee-slope eddy, fire weather, fire spread, bushfire risk management, high-country fire.*

1. INTRODUCTION

In rugged terrain the interaction of broad-scale atmospheric flows with the topography can produce surface wind fields that are highly variable in space and time. Modelling these dynamic surface winds is an important and challenging problem with applications in areas such as light and recreational aviation, pollutant dispersion modelling and modelling bushfire spread in complex terrain. Terrain-induced flows can also affect the local climatology in general.

Bushfire spread modelling typically combines information on surface winds with other meteorological variables, landscape attributes and fire behaviour models to provide guidance to those concerned with fire management on the likely spread of a fire under certain conditions, thereby facilitating the better deployment of resources during fire suppression activities. Fire spread modelling can also be used as part of longer-term fire management and risk planning, enabling more targeted fuel reduction strategies, for example.

To accurately simulate the spread of a fire, it is desirable to use wind speed and direction data that matches the actual conditions on a fire-ground as closely as possible. However, given the difficulty of predicting surface wind fields in general, common practice has been to simply extrapolate wind direction data from the closest source of meteorological information. In the most simple of these approaches wind speed and direction are assumed constant over the entire fire-ground. While this assumption may be appropriate over flat or gently undulating terrain, applying such a simplistic approach in rugged terrain can lead to serious errors in assessing the likely spread of a fire. Specifically, the assumption of constant wind speed and direction fails to recognise the nonlinear or turbulent effects that the terrain can have on local winds. Examples of such effects include eddy winds, thermally-driven winds and dynamic channelling. Thermally-driven winds can dominate surface wind patterns when bulk winds are light, while eddy winds and dynamic channelling, in particular, have been identified as efficient mechanisms for the development of large fires in rugged terrain (Byron-Scott, 1990; Whiteman, 2000; Kossmann et al., 2001). An example of the effects of channelling and eddy winds on fire behaviour and spread can be seen in figure 1.

In essence, the effects described above can all result in directional changes in the local wind field, which can then differ from the ambient wind direction by up to 90°, in the case of channelling, or 180° in the case of eddy and thermally-driven winds. Unexpected wind changes of such magnitudes can seriously compromise fire suppression activities and fire-crew safety. Understanding the intricacies of rugged terrain-wind systems is therefore an important part of understanding the associated fire regime and can improve the safety and effectiveness of fire management strategies.

To address the problem of accurately modelling fire spread in rugged terrain, more sophisticated fire spread models incorporate components designed to make local modifications to surface winds based on topographic considerations. A number of methods have been employed (Forthofer, 2007):

- CFD methods: simulating the surface wind field using computational fluid dynamics and the terrain surface as a boundary for the problem.
- Mass continuity methods: simulating surface wind fields using the equations of conservation of mass and the terrain surface as a boundary for the problem.
- Look-up tables: adjusting the surface wind field using a table of correction factors that depend on topographic aspect and ambient wind direction, or other simple rules of thumb.

Modelling surface wind fields using CFD methods can produce accurate information on surface wind fields but has the disadvantage of being computationally intensive requiring resources that may not be available to the average fire management agency. Mass continuity methods have the disadvantage of not accurately reproducing changes in wind direction caused by turbulent and thermal effects. Likewise, the simplistic
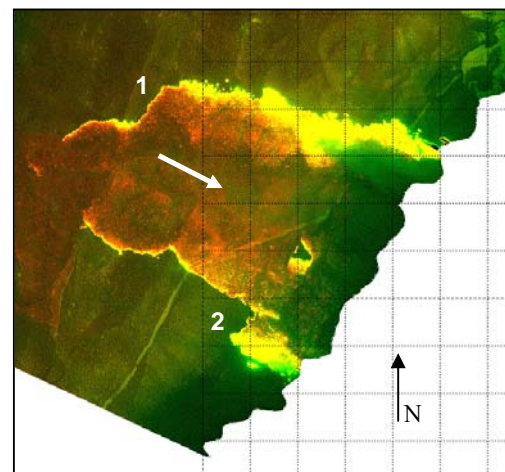

Figure 1. Multispectral linescan image of the Broken Cart fire at 15:09 18th January 2003. The bulk winds were from the west-northwest (white arrow). Sections of the northern and southern flanks that intersect lee slopes are spreading laterally (as indicated by the near right-angled kinks in the fire perimeter marked 1 and 2). Lateral and downwind spotting is evident with large tracts of land being rapidly set alight.

1 nature of methods employing look-up tables can fail to capture directional changes due to nonlinear and
2 thermal effects.

3 In this paper we discuss an empirical approach to understanding the directional component of a particular
4 wind-terrain system, based on probabilistic analysis of wind direction data collected by the authors. The
5 approach focuses on the probability distributions of wind direction data for a number of different paired
6 locations, and is an extension of an approach used by Whiteman and Doran (1993) to analyse the relationship
7 between synoptic-scale winds and winds in a mesoscale valley.

8 ## 2. DATA AND METHODS

9 The data for this study was collected within Tidbinbilla Nature Park, which forms part of the mountainous
10 region in the southwest Australian Capital Territory. The particular area was chosen for its complex
11 topography and the fact that it had experienced severe fire behaviour during the January 2003 alpine fires,
12 which had removed a lot of the natural forest canopy.

13 Four portable automatic weather stations were deployed in a transect along a steep slope to the east of a
14 prominent ridge known as 'Camel Back', with a relief of approximately 500-600m. The ridge is aligned
15 roughly in a north-south direction. Wind veins and cup anemometers were deployed at a height of 5 metres
16 above the ground surface and were programmed to collect data over 30 minute or 1 hour intervals between
17 December 2006 and October 2007, with wind directions given in terms of the sixteen standard points of the
18 compass rose. Where possible the stations were deployed at sites with very little or no canopy so that the
19 effects of the canopy on the wind data could be minimised. The four locations of the portable automatic
20 weather stations will be denoted A1, A2, A3 and A4. A map showing the locations and the underlying
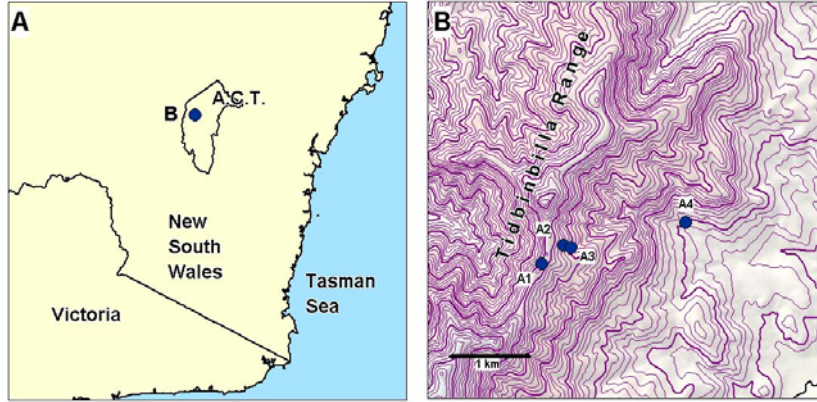21 topography can be seen in figure 2.

Figure 2. Location of study region and placement of portable automatic weather stations with respect to topographic features.

22 In the analyses we consider data from selected pairs of stations across the landscape. In what follows we will
23 take the first station to be the ridge-top station at A1, which is indicative of the ambient or bulk wind
24 direction, while the second station will be located at one of A2-A4, indicative of the terrain-modified wind
25 direction. We denote the wind direction experienced at A1 by θ_1, and the wind direction at AX by θ_X, where
26 X=2, 3, 4 and $0^o \leq \theta_1, \theta_X \leq 360^o$.

27 The ordered pair $\mathbf{p} = (\theta_1, \theta_X)$, X=2, 3 or 4, can be thought of as a state variable for the joint wind direction
28 system for the two station locations A1 and AX. To gain an understanding of the stochastic nature of the joint
29 wind direction system for the two locations in question, it is natural to consider their joint wind direction
30 distribution. To construct the joint wind direction distribution we took data recorded at A1 and AX and
31 matched wind direction records according to date and time. We denote the set of ordered pairs as P_X, and
32 suppose that P_X contains M_X ordered pairs of wind direction data. That is,

33 $$P_X = \left\{ \mathbf{p}^i = (\theta_1^i, \theta_X^i) : i = 1, \ldots, M_X \right\}.$$

34 Throughout this paper we will use the compass points N, NNE, NE, etc. interchangeably with their
35 corresponding values in degrees 0°, 22.5^o, 45°, etc. Hence, the ordered pair (WNW, SE) is the same as
36 $(292.5^o, 135.0^o)$.

1 Since the sampled wind direction data is given in terms of the sixteen standard compass points, it is natural to
2 consider the 17×17 grid whose lower left vertices are given by the vectors $\mathbf{a}_{jk} = (22.5^{o}(j - 1), 22.5^{o}(k - 1))$,
3 with $j, k = 1, \ldots, 17$.

4 This natural domain for the ordered pair $\mathbf{p} = (\theta_1, \theta_X)$ is the torus $T^2 = S^1 \times S^1$. The joint wind direction
5 distribution is simply the distribution of $\mathbf{p}$ over T^2. To ensure the correct toroidal topology we identify the
6 two sets of opposing edges of the grid $\{\mathbf{a}_{jk}\}$.

7 A discrete realisation of the joint wind direction distribution for a pair of stations is then given by the grid-
8 based function

9
$$H_{jk} = \sum_{i=1}^{M} \delta_{jk}^{i}, \quad j,k = 1,\ldots,17 \quad \text{where} \quad \delta_{jk}^{i} = \begin{cases} 1 & \text{if} \quad \mathbf{p}^i = \mathbf{a}_{jk} \\ 0 & \text{otherwise} \end{cases} \tag{2}$$

10 We will refer to H_{jk} as the sampled joint wind direction histogram
11 for the relevant pair of stations.

12 Given the inherent uncertainties in the data and sources of error
13 associated with field data collection, the sampled histograms
14 provided by equation (2) should not be considered to be without
15 some form of error. We therefore assume that H_{jk} is a noisy
16 realisation of a continuous joint wind direction distribution
17 function, that is

18
$$H_{jk} = g(\mathbf{a}_{jk}) + \varepsilon_{jk}, \quad j,k = 1,\ldots,17,$$

19 where g is the continuous (actual) joint wind direction distribution
20 function and ε_{jk} is a random error term assumed to be normally
21 distributed with zero mean.

22 To obtain a more robust estimate of the joint wind direction
23 distribution we use the method of thin-plate smoothing splines
24 (Wahba, 1990). The second-order thin-plate smoothing spline
25 estimate of the joint wind direction distribution function g is
26 obtained by minimising

27
$$\frac{1}{n} \sum_{j=1}^{17} \sum_{k=1}^{17} \left[H_{jk} - f(\mathbf{a}_{jk}) \right]^2 + \lambda J_2(f) \tag{3}$$

28 over a class of suitably smooth candidate functions f (Wahba,
29 1990). Here $n = 289$, the number of cells in the grid $\{\mathbf{a}_{jk}\}$, λ is a
30 smoothing parameter and $J_2(f)$ is the second-order roughness
31 penalty consisting of the integral of squared second-order partial
32 derivatives of f.

33 Due to the measures taken previously, to ensure the toroidal
34 topology of the initial grid, the fitted surfaces possess a structure
35 that is approximately toroidal. We assumed that the final surfaces
36 were scaled so that the total volume contained under each was
37 equal to unity. Each surface can then be interpreted as an estimate
38 of the joint probability distribution for the ordered pair $\mathbf{p} = (\theta_1, \theta_X)$
39 over the torus T^2.

40 To investigate the effect of wind speed on the various wind-terrain
41 systems the analyses described above were repeated using a
42 number of threshold wind speeds. In these analyses, the wind
43 direction pair was only included in the histogram totals if the
44 simultaneous wind speed at A1 was greater than or equal to the
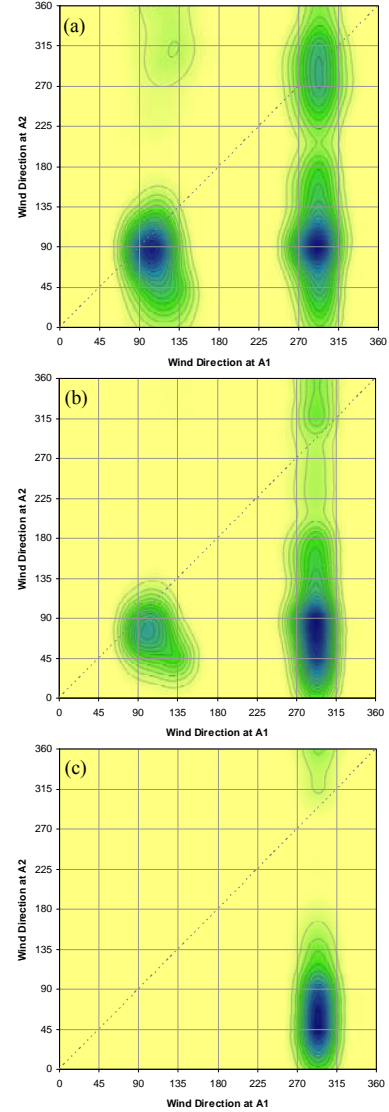45 threshold wind speed. The threshold wind speeds used were 0, 2,
46 4, 6, 8 and 10 ms^{-1}.

Figure 3. Wind direction distributions for the (A1, A2) pairing. (a) $U_{A1} \geq 0$ ms^{-1}, (b) $U_{A1} \geq 4$ ms^{-1} and (c) $U_{A1} \geq 8$ ms^{-1}.

1 **3. RESULTS**

2 In the following we will use U_{A1} to denote the wind speed at the location A1, and U_{AX} to denote the wind
3 speed at the locations AX, X=2, 3, 4.

4 **3.1. (A1, A2) pairing**

5 Figure 3 shows the joint wind direction distributions for the (A1, A2) pairing for threshold wind speeds of 0,
6 4 and 8 ms^{-1}. All exhibit a definite modal structure. The joint distribution corresponding to all matched pairs
7 (i.e. $U_{A1} \geq 0$ ms^{-1}), exhibits four modes located roughly at (WNW, E), (ESE, E), (WNW, WNW) and (SE,
8 NW). To facilitate analysis the (WNW, E) mode was defined as $245^{o} \leq \theta_{A1} \leq 335^{o}$ and $0^{o} \leq \theta_{A2} \leq 210^{o}$, the
9 (ESE, E) mode was defined as $60^{o} \leq \theta_{A1} \leq 160^{o}$ and $0^{o} \leq \theta_{A2} \leq 160^{o}$, the (WNW, WNW) mode was defined as
10 $245^{o} \leq \theta_{A1} \leq 335^{o}$ and $210^{o} \leq \theta_{A2} \leq 360^{o}$ and the (SE, NW) mode was defined as $80^{o} \leq \theta_{A1} \leq 160^{o}$ and $260^{o} \leq$
11 $\theta_{A2} \leq 360^{o}$.

12 Increasing the threshold wind speed
13 changes the modal structure of the
14 corresponding joint distributions, as
15 can be seen in figure 3. Figure 4
16 illustrates how the modal probabilities
17 respond as the threshold wind speed is
18 varied. In particular, the mode at (SE,
19 NW) has completely vanished when
20 $U_{A1} \geq 4$ ms^{-1}. The dates and times
21 corresponding to the (SE, NW) mode

Figure 4. Response of modal probabilities for the (A1, A2)
pairing as the threshold wind speed is varied.

22 indicated that such conditions occur
23 preferentially during the night-time. In
24 fact it was found that only about 4% of events corresponding to the (SE, NW) mode occurred between 08:00
25 and 16:00 hours. Hence the (SE, NW) mode, and its disappearance as the threshold wind speed is increased,
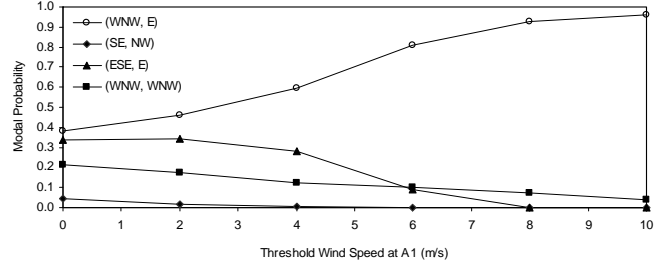26 is consistent with the occurrence of a weak nocturnal drainage flow, which is overcome by stronger ambient
27 winds.

28 As the threshold wind speed is increased the (WNW, E) mode dominates. The likelihood associated with the
29 (WNW, WNW) mode drops substantially for $U_{A1} \geq 4$ ms^{-1} with a complementary rise in the likelihood of the
30 (WNW, E) mode. In fact as the wind speed threshold rises above 8 ms^{-1} the joint wind direction distribution
31 becomes unimodal at (WNW, E). The fact that this mode dominates for high wind speeds across the ridge at
32 A1 is interesting as it indicates that the winds at A1 and A2 are often opposed, despite the fact that they are
33 within a few hundred metres of each other. Figure 3c implies that when a WNW wind of 8 ms^{-1} or more is
34 flowing across the ridge at A1, the wind direction at A2 can be anywhere between 0° and 180° with a high
35 likelihood of it falling between NNE and ESE.

36 It is well known that diurnal heating and cooling of rugged landscapes can induce thermal winds that flow
37 downslope just after sunset and upslope at sunrise (Whiteman, 2000). It is therefore possible that the (WNW,
38 E) mode could be due to thermally-driven upslope winds. Such winds would be expected to be slight and
39 occur during daylight hours. An examination of the dates and times corresponding to (WNW, E) mode,
40 however, suggests that this mode is not entirely due to thermal effects. The dates and times indicated that that

41 the winds at A1 and A2 can be
42 opposed for extended periods of up
43 to 5 or 6 days, and that these
44 extended events mostly occurred
45 for higher wind speeds. It is
46 therefore more likely that these
47 data correspond to the occurrence
48 of a lee-slope eddy. The distended
49 shape of the (WNW, E) mode in
50 figure 3 suggest that these thermal
51 and eddy-driven winds can also
52 have an across slope component at
53 times, which in the case of an eddy
54 wind, would imply an overall
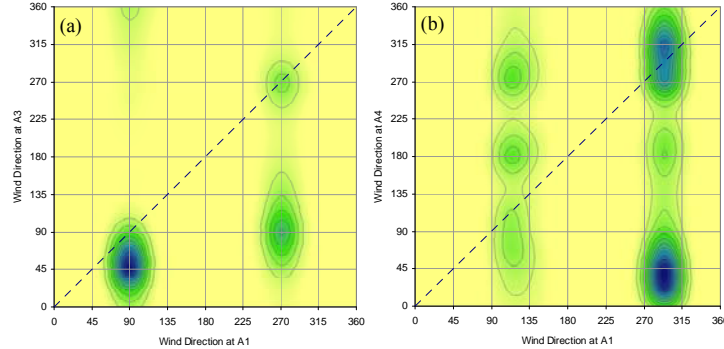55 helical motion above the slope.

Figure 5. Joint wind direction distributions for (a) the (A1, A3) pairing
and (b) the (A1, A4) pairing, assuming a threshold wind speed of $U_{A1} \geq$
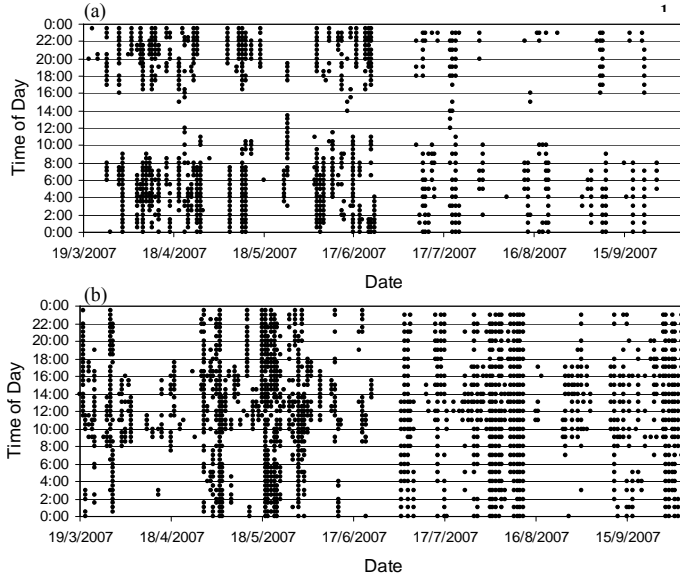2 ms^{-1}.

Figure 6. (a) Plot of time of day against date for data contributing to the (ESE, W) mode, (b) Plot of time of day against date for data contributing to the (WNW, NE) mode. All matched pairs have been included (i.e. $U_{A1} \geq 0$ ms^{-1}).

3.2. (A1, A3) and (A1, A4) pairings

Joint wind direction distributions for the (A1, A3) and (A1, A4) pairings can be seen in figure 5. For brevity, only the distributions corresponding to $U_{A1} \geq 2$ ms^{-1} are shown. The distributions for the (A1, A3) pairing were quite similar in structure to those for the (A1, A2) pairing. In particular, the distributions for the (A1, A3) pairing also indicated a high likelihood of wind reversal at A3 when it is on the lee side of the ridge. This indicates that the methods used are reasonably robust since the locations A2 and A3 are only approximately 60m apart. The differences in the horizontal position of the modes for the (A1, A2) and (A1, A3) pairings are due to the different sampling periods at A2 and A3.

The joint wind direction distributions for the (A1, A4) pairing exhibit six identifiable modes, indicating a more complicated wind-terrain interaction.

26 Figure 6a shows the dates and times corresponding to the data pairs in the (ESE, W) mode, i.e. $75° \leq \theta_{A1} \leq$
27 $165°$ and $232° \leq \theta_{A4} \leq 352°$. As can be seen, the majority of data pairs in the (ESE, W) mode occur between
28 16:00 hours and 09:00 hours, which is consistent with them being caused by a nocturnal drainage flow. By
29 contrast, the dates and times corresponding to data pairs in the (WNW, NE) mode follow quite a different
30 pattern. Figure 6b indicates that conditions contributing to the (WNW, NE) mode often occurred during
31 daylight hours, but could persist for several days. The pattern in figure 6b is similar to that exhibited by the
32 dates and times corresponding to the (WNW, E) mode for the (A1, A2) pairing.

33 A comparison of the dates and times corresponding to the (WNW, NE) mode for the (A1, A4) pairing and the
34 (WNW, E) mode for the (A1, A2) pairing indicated that there was a high degree of coincidence. This is a
35 strong indication that these analogous modes arise as a consequence of the same processes, most likely
36 upslope thermal winds and lee eddies.

37 The additional modes for the (A1, A4) pairing, located at (ESE, S) and (WNW, S), indicate the likelihood of
38 differences in wind direction of approximately $90°$ at A1 and A4. Examination of the dates and times
39 corresponding to the (WNW, S) mode indicated that such conditions occurred preferentially during daylight
40 hours (approx. 10:00-18:00 hours) with only sporadic and fleeting events taking place in the night. The
41 timing of these events suggests the existence of a thermal upslope wind from the south at A4. This is
42 plausible since there is a spur with a steep southerly-facing sidewall just to the north of A4, which could
43 provide the thermal differences required to produce such a flow. The dates and times corresponding to the
44 (ESE, S) mode exhibited a slight preference for daytime occurrence, again consistent with a thermal upslope
45 wind, but also indicated that conditions in this mode can persist for a day or two. This suggests that these
46 persistent conditions are not linked with any diurnal process. Further examination of the dates and times
47 showed that it was mostly these persistent events that were contributing to the (ESE, S) mode for higher
48 threshold wind speeds. Forced channelling of the bulk east-south-easterlies is a likely cause for these types of
49 persistent events.

50 **4. DISCUSSION AND CONCLUSIONS**

51 A probabilistic analysis of measured data from the wind-terrain system corresponding to a steep slope has
52 been presented. The analysis focused on the structure of joint wind direction distributions for pairs of
53 locations; one relating to the ambient or bulk wind direction and one relating to the terrain-modified wind.
54 The joint distributions exhibited distinct modal structures, indicating preferences for certain regions of the
55 toroidal state space. Analysis of the timing of conditions corresponding to specific modes provided strong
56 evidence for the existence of several different processes. These processes included thermally-driven upslope

winds during the day and complementary down-slope winds during the night-time, forced channelling and lee-slope eddies.

As the threshold wind speeds were increased, different modes responded in different ways. In particular, modes corresponding to processes such as channelling and lee-slope eddies were more dominant for higher wind speeds. This is not surprising since when the winds are strong, mechanical-fluid effects would tend to overpower the weaker thermal effects.

The similarity of the results for different locations suggest that they could be extrapolated with reasonable accuracy to other steep slopes, particularly in regions that experience a similar bimodal ambient wind direction distribution that aligns with topography in a similar way. At the least, the result should cause fire managers to view lee-slopes, and the regions downwind, with caution, particularly when the ambient winds are over 8 ms^{-1} (approx. 30 km h^{-1}).

The analyses revealed the distinctly stochastic nature of the wind direction data. Given a fixed ambient wind direction it does not seem possible to uniquely specify a corresponding terrain-modified wind direction with complete certainty. This suggests that a more probabilistic approach to the problem is appropriate; rather than specifying a wind direction, it should be sampled from the relevant distribution. Moreover, the results cast doubt upon the utility of deterministic methods employed to estimate terrain modified wind fields in rugged terrain. In particular, methods that don't account for thermal and turbulent effects could be in error more than 75% of the time when applied to steep lee-slopes. A probabilistic approach such as the one outlined is also likely to be more suitable for risk based studies, especially those that use Monte Carlo or ensemble approaches to model bushfire risk.

The majority of the modes observed in the joint wind distributions are located around specific points on the $S^1 \times S^1$ torus (for example, (E, W)). In a dynamical systems sense, these points could perhaps be interpreted as attractors for the local meteorology. Investigating a suitable low dimensional system to verify this would be an interesting theoretical extension of the study presented.

ACKNOWLEDGEMENTS

REFERENCES

Byron-Scott, R.A.D. (1990) The effects of ridge-top and lee-slope fires upon rotor motions in the lee of a steep ridge. *Mathematical and Computer Modelling*, 13, 103-112.

Forthofer, J.M. (2007) *Modeling Wind in Complex Terrain for Use in Fire Spread Prediction*, Master's Thesis, Colorado State University, Fort Collins, CO.

Kossmann, M., A. Sturman, and P. Zawar-Reza, (2001) Atmospheric influences on bushfire propagation and smoke dispersion over complex terrain. In: *Proceedings of the Australasian Bushfire Conference*, 3-6 July 2001. Christchurch, New Zealand.

Wahba, G. (1990) *Spline Models for Observational Data*. CBMS-NSF Regional Conference Series in Applied Mathematics. SIAM Philadelphia.

Whiteman, C.D., and J.C. Doran, (1993) The relationship between overlying synoptic-scale flows and winds within a valley. *Journal of Applied Meteorology*, 32, 1669-1682.

Whiteman, C.D. (2000) *Mountain meteorology fundamentals and applications*. Oxford University Press, New York.